A steady-state Eulerian-Lagrangian solver for non-reactive sprays

A. Andreini, C. Bianchini, B. Facchini, A. Giusti*
Dipartimento di Energetica Sergio Stecco, University of Florence, Italy
andrea.giusti@htc.de.unifi.it

Abstract

A steady-state RANS solver for sprays, based on fully coupled Eulerian-Lagrangian approach, was implemented in the framework of the open source CFD code called OpenFOAM. Because of the intrinsic unsteady nature of the Lagrangian tracking, the most straightforward approach to solve for droplet motion in continuous media is the fully unsteady method. However, since for many industrial purposes the focus is on the time averaged solution, steady state acceleration techniques are of primary interest.

The computational strategy, implemented to handle typical configurations encountered in liquid-fueled gas turbine combustors such as pressure swirler atomizers, consists in separately resolving the gas and the liquid phases exploiting respectively a standard steady-state pressure based solver and a pseudo-transient Lagrangian approach. The coupling between the two phases is achieved by means of time averaged source terms in the Eulerian conservation equations and by including gas-droplet interaction in the Lagrangian tracking to account for evaporation, drag, break-up and turbulent dispersion. The Lagrangian tracking is performed using a statistically representative number of parcels which are tracked over their entire history from injection up to either evaporation or computational domain exiting. Pseudo time integration employs a user-defined time-step chosen to obtain an optimal fuel mass injection to suitably represent droplet distribution. The obtained instantaneous solutions are then summed up to compute the Lagrangian solution and hence the steady-state spray-gas coupling source terms. In such a way the number of parcels necessary to describe the spray evolution, as well as the computational time to resolve the Lagrangian tracking of the liquid particles, is strongly reduced compared to standard unsteady approaches. In order to improve the stability of the coupling source terms, an averaging procedure among successive Lagrangian solutions is proposed instead of the classical approach which only considers the last available Lagrangian solution. Such averaging is performed using a moving average approach which only accounts for a given number of Lagrangian solutions. This technique allows us to increase the number of parcels considered in source term computation without increasing the computational efforts and to smooth out possible oscillations of the Lagrangian solution.

This paper describes the derivation and implementation of such numerical methods. Solver validation was performed against experimental data available from two well known literature test cases. The first one consists of an isothermal swirled flow with solid particles axially injected at the center of the vortical structure. In this case, the Eulerian-Lagrangian coupling is reduced to flow field interactions, thus only drag, particle dispersion caused by turbulence and turbulence generated by particle motion are to be considered. The solution obtained with the proposed coupling approach was compared with experimental measurements and numerical results obtained using classical approaches: detailed results in terms of gas phase velocity field, particle velocity and particle size-velocity correlation are presented. The second test case is an isopropyl alcohol spray generated by a hollow cone injector issuing into a co-flowing heated air stream. In this case the Eulerian-Lagrangian coupling is also extended to the mass and energy conservation equations and the convergence capabilities of the different approaches are further tested. Comparisons with experiments for both continuous and disperse phase are reported.

The newly implemented solver showed faster convergence rates compared to numerical approaches already available in the code, maintaining equivalent capabilities for mean flow field and particle distribution prediction.

Introduction

Liquid sprays are used in many industrial applications and mechanical devices. In order to design such devices or simply to understand their behaviour, it is often required to exploit proper tools able to describe spray evolution and its interaction with the main flow. As far as fluid flow is concerned, the CFD is becoming increasingly important also in industrial design processes. It follows that the development and setup of numerical tools able to catch the main flow features in reasonable time is of great interest. Multiphase flows involving sprays are very complex since many simultaneous physical processes have to be accounted for, e.g. primary and secondary breakup, interaction between droplets and turbulence, heat and mass transfer between particles and gas-phase, interaction of particles with each other. Several numerical methods can be used to simulate dispersed sprays

*Corresponding author: andrea.giusti@htc.de.unifi.it

[2]; the most popular method is probably the Eulerian-Lagrangian approach where gas-phase is modeled as a continuum and solved following the Eulerian approach while particles are treated as discrete entities and tracked over the computational domain using a Lagrangian formulation. Interaction between gas-phase and particles is taken into account by means of simple models directly derived from basic physical principles and this formulation is suited for both dilute and dense sprays. The main drawback of this approach is related to the high number of droplets that are required to have statistically representative solutions that generally makes computational costs grow above affordable levels for industrial applications. In order to reduce computational costs, droplets are usually represented by numerical parcels, that is groups of droplets with the same properties. The dispersed phase can also be modeled as a continuum in the so called Eulerian-Eulerian approach. This method is usually less time consuming, however it introduces many inaccuracies, basically related to the continuum hypothesis which does not allow different droplets to be distinguished from each other, which may not always be tolerable [6]. Another possible approach, the Probability Density Function method, uses a joint PDF transport equation to statistically describe the spray evolution [8]. The main advantage of the PDF approach is the ability to provide accurate droplets statistics in the whole domain whereas the Eulerian-Lagrangian approach gives reliable results only in those regions with high droplets concentrations; however it requires a huge computational cost. It should be noted that the previous classification is not exhaustive and other computational methods could be adopted.

This work deals with the Eulerian-Lagrangian approach focusing in particular on an innovative strategy to couple droplet tracking to a steady-state continuous media solver. Despite the unsteady nature of droplet motion making the fully unsteady method the most straightforward way to model their behaviour, in many cases the industrial interest is on time-averaged quantities. The proposal of steady-state acceleration techniques for both reacting and non-reacting sprays is hence of primary interest. In case of steady state assumption, convergence of Eulerian-Lagrangian coupling could become an issue and the choice of a convergence criteria is not straightforward. The reason is mainly related to the Eulerian-Lagrangian coupling source term fluctuations due to the stochastic formulation of many models describing the spray evolution, for example injection and turbulent dispersion models. In order to enhance numerical stability, under-relaxation of source terms is generally implemented [2], alternatively this work proposes a moving average technique to damp possible oscillations. In the following sections a comprehensive description of the implementation of the proposed solver is reported as well as the results obtained for two different test cases and their comparison with experimental and other computations data.

Numerical Methods

As stated before, when the Eulerian-Lagrangian approach is used, the gas-phase is considered as a continuum and solved with Eulerian methods while the particle dynamics is simulated using a Lagrangian tracking.

Droplet motion

The spray is numerically represented by a cloud of parcels, where a parcel is a group of droplets with the same physical characteristics. Before describing the basic equations used in the Lagrangian tracking, let's recall basic assumptions on which the motion equation is based. First of all the spray is assumed diluted and droplets are considered non deformable and non rotating. Generally droplets are treated as spherical with non-sphericity accounted for by means of specific correction factors. Since the rotational speed is neglected, the particle dynamics is simply described by the Newton's second law which expresses a balance between forces acting upon a particle and its acceleration:

$$\frac{d\mathbf{u}_p}{dt} = \sum_i \mathbf{F}_i \tag{1}$$

where $\mathbf{u}_p$ is the particle velocity and $\mathbf{F}_i$ represents a general force (per unit of mass) acting upon the particle. In the implemented model, particle motion is determined only by drag, gravitation and buoyancy forces. In this case Equation (1) becomes:

$$\frac{d\mathbf{u}_p}{dt} = \frac{3}{4}\frac{\rho}{d_p\rho_p}C_D\left(\mathbf{u}-\mathbf{u}_p\right)\|\mathbf{u}-\mathbf{u}_p\| + \frac{\rho_p-\rho}{\rho_p}\mathbf{g} \tag{2}$$

where C_D is the drag coefficient based on correlations for spheres, ρ_p is the particle density, d_p is the particle diameter, $\mathbf{u}$ and ρ are respectively the velocity and the density of the gas-phase, $\mathbf{g}$ is the gravitational acceleration. All the other forces were neglected, in particular virtual mass, Basset, Saffman and Magnus forces [5, 3]. Basset forces are unsteady interactions due to acceleration of relative velocity between particle and gas-phase and for liquid or solid particles these forces could usually be neglected. The Saffman forces are related to the velocity gradients in the gas-phase and their effect could be important only in the injection zone and in regions close to the

walls [7]. Finally, Magnus forces are generated by particle rotation and they are usually much smaller than drag forces.

During its life, a droplet may undergo heat transfer, evaporation, secondary breakup and interaction with turbulence of the gas-phase both in terms of influence of turbulence on particle motion and turbulence induced by the particle itself. In the present work, evaporation process is modeled using the uniform temperature model described in [1], heat transfer has been described using the Ranz-Marshall correlation [11] whereas the effect of turbulence on the particle motion is accounted for by means of a stochastic turbulent dispersion model as introduced by [4].

The Lagrangian tracking is performed following the approach described in [4]. A statistically representative number N_p of parcels is injected and their trajectories are computed by numerically integrating Equation (2). Droplet injection is modeled by assigning droplet mass flow rate $\dot{m}_p$; thus, the total mass M_p of the representative sample is obtained starting from the Lagrangian time step by giving the number of time steps in which parcels are injected. The Lagrangian tracking starts from the injection location and proceeds until parcels either leave the domain or completely evaporate. The particle field in the whole domain is obtained by summing up the Lagrangian solution at each integration step; in other words the entire history of the N_p parcels during the Lagrangian tracking is recorded. It is important to note that the assigned integration time step is actually decomposed into sub-integration time steps according to the relaxation times that characterize the physical phenomena related to droplet motion (heat transfer, boiling, drag and so on).

Gas-phase field

The mathematical model for the continuous gas phase is represented by the Navier-Stokes equations, which state the laws of conservation of mass, momentum and energy, with additional simplifications due to steady-state and further assumptions on fluid properties such as ideal gas equation of state, Newtonian modelling for viscous forces and constant transport properties. The effects of turbulence on the time-averaged solution are taken into account by means of Favre averaging and closure of the Reynolds stress tensor is achieved exploiting the $\mathrm{k}-\omega$ SST model [9].

The solver employed is a pure steady-state pressure-based solver exploiting SIMPLE loop [10] to solve for the pressure velocity coupling. Density variations are accounted for by solving the energy equation in terms of static enthalpy and assuming ideal gas behaviour. Finite-volume discretization is achieved by means of Total Variation Diminishing schemes for the convective terms and central differencing for the diffusive terms. Under-relaxation technique is used to enhance the algorithm stability. The coupling terms with the Lagrangian solution appear in the discretized equations as explicit source terms S_p on the RHS.

Coupling strategy

The overall solution procedure consists in repeatedly solve disperse and continuous phase using the approaches described in previous sections. A basic iteration cycle could be considered composed by two different steps. First of all the Lagrangian tracking is performed using the most updated Eulerian flow field available. When a parcel traverses a cell, mass, momentum and energy source terms are recorded and averaged with the source terms released by all the other particles. Thus, at the i-th Lagrangian tracking, source terms in a generic cell are computed as:

$$S_p^{(i)} = \frac{\dot{m}_p}{M_p} \sum_{k=1}^{\hat{N}} s_{p,k}^{(i)} \tag{3}$$

where $\hat{N}$ is the cumulative number of parcels traversing a cell and $s_{p,k}^{(i)}$ is the contribution of the k-th parcel to the source term computation. Then source terms are passed to the gas-phase and held constant during Eulerian computation. The update of the coupling source terms is generally performed only after the under-relaxed Eulerian fields are solved a certain amount of times.

As mentioned before, when the steady state formulation is considered, it is often important to use under-relaxation techniques in order to improve the computation stability. In this paper a method based on moving average is proposed. From a purely mathematical point of view, the approach consists in calculating source terms to be assigned to the Eulerian solver by averaging the last $\bar{N}$ solutions of the Lagrangian tracking. $\bar{N}$ should be large enough to smooth fluctuations of source terms and thus to obtain a really representative mean value. Let's consider the i-th Lagrangian iteration. Mean source terms at the end of the iteration are computed as:

$$\bar{S}_p^{(i)} = \frac{1}{\bar{N}} \sum_{k=i-\bar{N}+1}^{i} S_p^{(k)} \tag{4}$$

Table 1. Air flow and particle conditions (*Test 1*)

Air flow	
Mass flow rate of primary jet	9.9 $\mathrm{g/s}$
Mass flow rate of secondary jet	38.3 $\mathrm{g/s}$
Inlet Reynolds number (D=64 mm)	52400
Swirl number	0.47
Particles	
Particle mean number diameter	45.5 $\mu\mathrm{m}$
Particle material density	2500 $\mathrm{kg/m^3}$
Particle mass flow rate	0.34 $\mathrm{g/s}$

Figure 1. Test case scheme (*Test 1*).

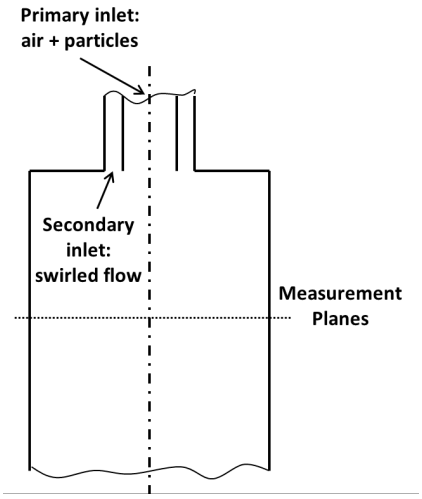

In this way the representative population is composed by all the parcels considered in the $\bar{N}$ iterations. The moving average has been numerically implemented using the following strategy to save allocated memory. Besides $\bar{S}_p^{(i)}$ another mean value $\bar{S}_{\bar{N}/2}$ is computed. It represents the mean source terms in $\bar{N}/2$ Lagrangian iterations and this value is updated every $\bar{N}/2$ Lagrangian trackings. The moving average is evaluated as follows:

$$\bar{S}_p^{(i)} = \frac{1}{\bar{N}}(\bar{N}\bar{S}_p^{(i-1)} + S_p^{(i)} - \bar{S}_{\bar{N}/2}) \tag{5}$$

The use of this strategy to approximate the moving average allows us to not store all the data of the last $\bar{N}$ Lagrangian iterations but only two mean values. In particular the term $\bar{S}_{\bar{N}/2}$ allows us to avoid abrupt changes in source term values. Furthermore, in respect to a standard averaging procedure which considers all the Lagrangian iterations, the moving average approach let the effect of initial values be less significant; the sensibility to initial values could be further reduced by using a weighted moving average.

Validation

The solver has been validated against two different literature test cases. The first one considers the motion of solid particles in a swirled flow. Since solid particles are considered, interaction between gas-phase and droplets is reduced to drag forces and turbulent dispersion only (the turbulence induced by particle motion is not considered in the present study). In the second case evaporation in turbulent flows is considered, thus the coupling between continuous and disperse phases is extended to mass and energy exchanges.

Test 1

The first test case consists in an isothermal swirling particulate two-phase flow, experimentally investigated by Sommerfeld and Qiu [12]. Figure 1 schematically represents the experimental configuration, basically a vertical test section with two different flow circuits for the primary and secondary annular flows. Glass particles, with a given size distribution, move down from a reservoir and enter the measurement section together with the primary flow whereas a swirled flow issues from the secondary inlet. PDA measurements were performed at different planes normal to the main chamber axis. In Table 1 the main flow conditions are given; for geometrical features and all the other details see reference [12].

As shown in Figure 2, the experimental rig was modeled as a 90 degrees sector with cyclic boundary conditions on lateral faces. The computational domain was discretized by means of a multi-block hexahedral structured mesh of about 470000 elements. Fixed value velocity boundary condition was imposed in both primary and secondary inlet whereas a statistically representative population of 12500 parcels was injected at the main chamber entrance representing the experimental size distribution with a Rosin-Rammler function. As regards droplet-wall interaction, solid surfaces were modeled as reflecting walls.

Figure 3 shows a comparison between experimental and numerical 2D streamlines in an axial-radial plane; the extension of the recirculation zones is well predicted both in the centre and on the left corner.

In Figure 4 radial profiles of gas-phase axial and tangential mean velocities are reported at two different planes.

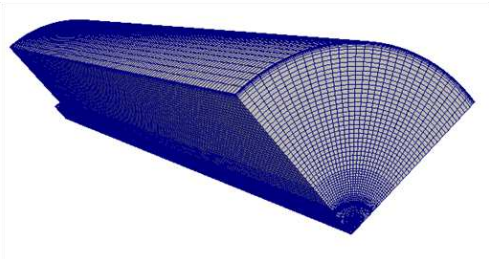

Figure 2. Computational mesh.

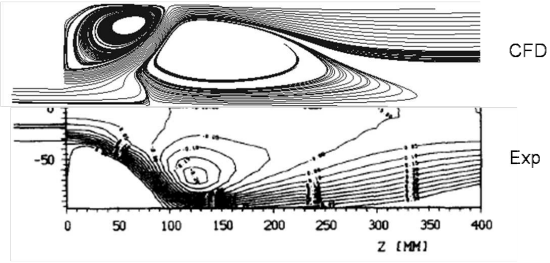

Figure 3. Comparison between numerical and experimental [12] stream lines.

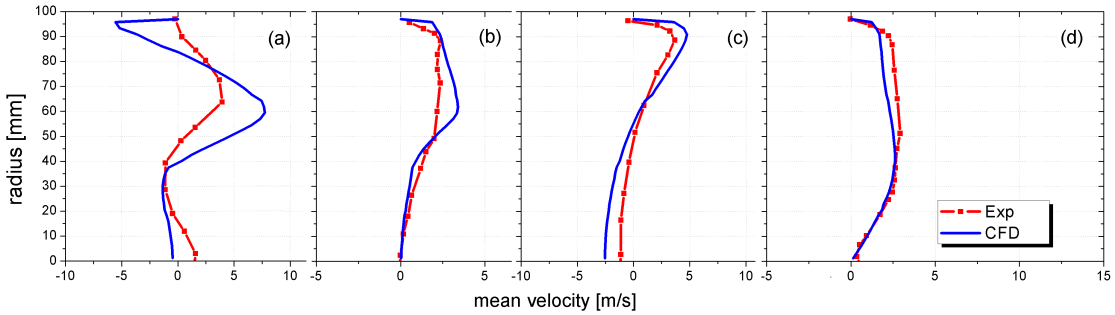

Figure 4. Gas-phase mean velocity profiles (*Test 1*): (a) mean axial velocity at plane z=85 mm, (b) mean tangential velocity at plane z=85 mm, (c) mean axial velocity at plane z=195 mm, (d) mean tangential velocity at plane z=195 mm.

A good agreement between experimental and numerical results is reached far away from the inlet while near the inlet some discrepancies arise. It should be noted that the same differences were also found by Chrigui in his thesis work [2] using $\mathrm{k}-\varepsilon$ turbulence model. Figure 5 shows how particle velocity profiles well reproduce experimental data at those locations where the gas-phase flow was well predicted. It is important to note that experimental measurements are referred to particular droplet size classes (30, 45, 60 μm) while numerical results consider all the particles together representing a mass averaged value.

In Figure 6 numerical results obtained with the implemented solver are compared with results obtained with the unsteady solver already present in the base version of OpenFOAM. The two different solvers gave the same mean velocity profiles, for both gas and disperse phase proving that, in case the interest is on time averaged quantities only, the use of a steady solver might substitute traditional unsteady solvers that are more computationally expensive. Both simulations were initialized using the RANS solution obtained from a simulation without particles; the unsteady solver needed a CPU time of about 3.3e+6 s for just keeping the particles from the inlet to the

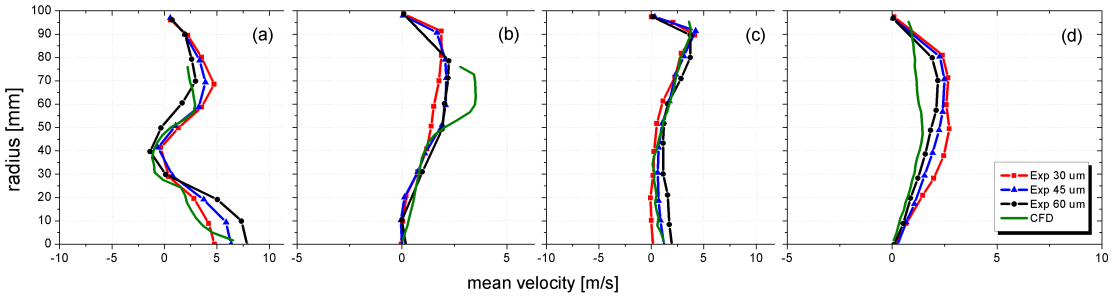

Figure 5. Particle mean velocity profiles (*Test 1*):(a) mean axial velocity at plane z=85 mm, (b) mean tangential velocity at plane z=85 mm, (c) mean axial velocity at plane z=195 mm, (d) mean tangential velocity at plane z=195 mm.

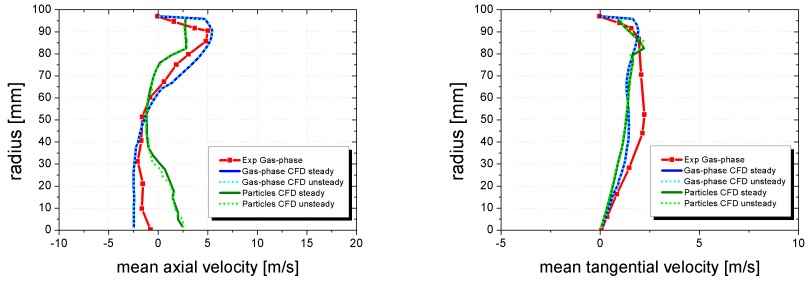

Figure 6. Comparison between steady state and unsteady solvers at plane z=112 mm (*Test 1*).

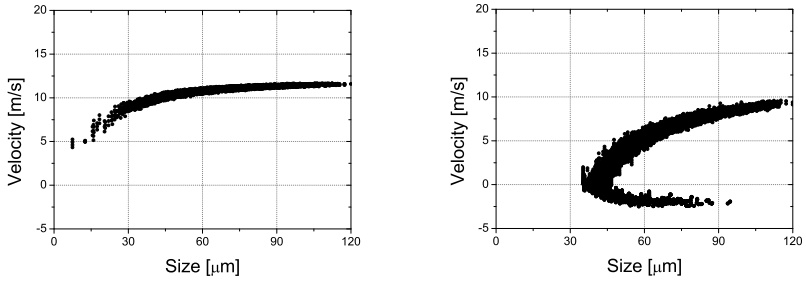

(a) Point (0.0 m, 0.0 m, 0.052 m) (b) Point (0.0 m, 0.0 m, 0.112 m)

Figure 7. Particles size-velocity correlations (*Test 1*).

outlet with a time step equal to 1.0e-6 s. Performing one Lagrangian tracking every ten Eulerian iterations, in the same time the steady state solver could complete about 5.2e+4 iterations; considering that approximately 1.0e+4 iterations were sufficient to reach convergence, the great advantage of the steady state solver is shown.

Finally, in Figure 7 two size-velocity correlation plots are reported at different points in the domain. Comparisons with experimental data [12, 13] showed that numerical results are less dispersed than experimental ones following the same trend observed in other works [13].

Test 2

The second test case that was simulated to evaluate the capabilities of the implemented solver considers evaporation of isopropyl alcohol in a turbulent environment. Figure 8 shows a schematic representation of the test rig experimentally investigated by Sommerfeld and Qiu [14]. It consists of a main cylindrical chamber where heated air is supplied through an annulus; droplets are injected at the centre of the annulus by means of a hollow cone injector. Geometrical details are given in reference [14] together with all flow conditions. Two different simulations were performed, without and with the presence of the spray. Table 2 summarizes the main flow parameters of such simulations.

The computational domain reproduces a 90 degrees sector of the test rig. A multi-block hexahedral structured mesh of about one million elements was used (see Figure 9). The inlet annular duct has been included in the computational domain in order to have a developed flow at the main chamber entrance. A fixed value velocity was imposed at air inlet, ambient pressure was set at the outlet and no-slip condition together with experimental temperature profile was imposed at walls. A representative population of 16000 parcels was used. Following

Table 2. Air flow and particle conditions (*Test 2*)

Case	Diameter nozzle holder [mm]	Air volume flow rate [m^3/s]	Air mass flow rate [g/s]	Maximum air velocity [m/s]	Maximum air temperature [°C]	Liquid mass flow rate [g/s]	Liquid temperature at nozzle exit [°C]
Single-phase flow	40	0.032	29.0	18.0	100	-	-
1	40	0.034	32.6	18.0	80	0.44	32

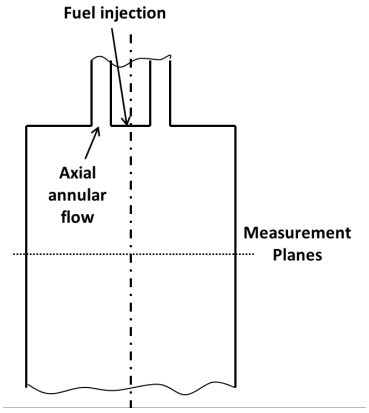

Figure 8. Test case scheme (*Test 2*).

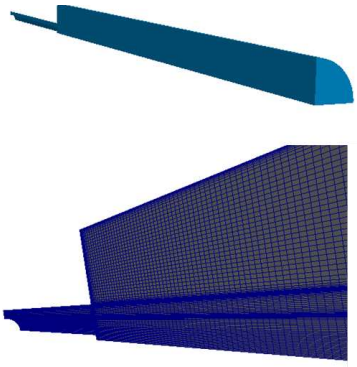

Figure 9. Computational domain and mesh (*Test 2*).

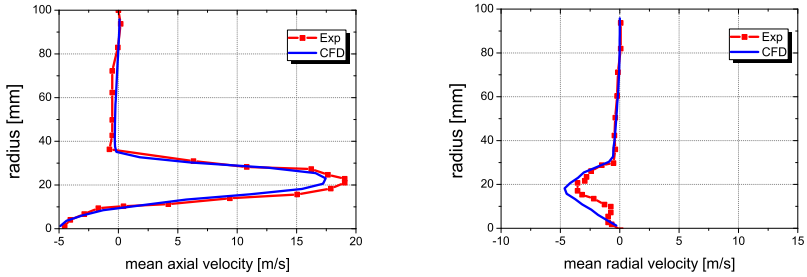

Figure 10. Mean velocity radial profiles at plane z=25 mm for single-phase flow (*Test 2*).

[2] particle injection was modeled with eight concentric injectors giving for each one droplet mean diameter and injection velocity. A reflecting wall condition was imposed at solid surfaces, the uniform temperature model [1] was used for droplet evaporation whereas neither coalescence nor secondary breakup model were considered. It is important to note that in the uniform temperature model, heat conduction inside the droplet is considered infinitely high, so no temperature gradients inside the droplet have to be solved reducing the computational effort.

Figure 10 shows a comparison between numerical results and experimental data of the case without spray in a plane normal to the main chamber axis. A good agreement was reached and similar results were also obtained in the other measurement planes. In Figures 11 and 12 results of the simulation with spray at two different planes are considered. Results obtained with the implemented steady-state solver have been compared with both experimental data and results obtained with Ansys CFX-13.0 using the same computational setup. A reasonable agreement between numerical simulation and experiments both in terms of axial velocity and particle diameter was obtained. Present results are also in good agreement with CFX simulation showing that the implemented code has an equivalent behaviour to one of the most common commercial codes. The two codes are almost equivalent also in terms of CPU time required by the simulation, with the implemented solver which shows slightly better convergence rates.

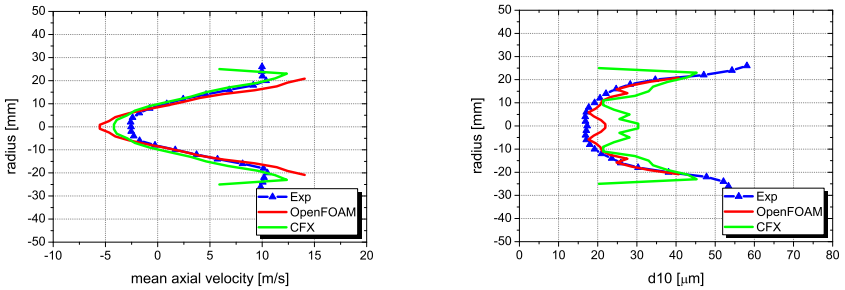

Figure 11. Particle mean axial velocity and diameter profiles at plane z=25 mm (*Test 2*).

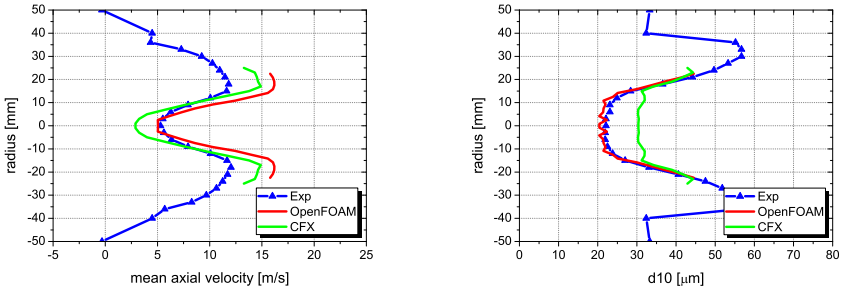

Figure 12. Particle mean axial velocity and diameter profiles at plane z=50 mm (*Test 2*).

Conclusions

A steady state Eulerian-Lagrangian solver for non-reactive sprays was implemented in the framework of the open source code called OpenFAOM exploiting a moving average approach in order to under-relax Eulerian-Lagrangian coupling source terms.

The performance of the implemented solver was evaluated by simulating two different literature test cases. Obtained results were compared with both available experimental data and other numerical simulations performed with unsteady solver and commercial codes. The implemented solver showed faster convergence rates compared to unsteady solver maintaining adequate capabilities in predicting time averaged fields for both gas phase and particles without any significant difference compared to steady state solvers available in commercial codes.

The solver is going to be integrated with suitable combustion models and chemical solvers so that simulations of typical liquid-fueled gas turbine combustors could be performed.

Acknowledgements

The research leading to these results has received funding from the European Union Seventh Framework Programme (FP7/2007-2013) under grant agreement n°265848 and was conducted within the FIRST project. The permission for the publication is gratefully acknowledged by the authors.

References

[1] Borman, G. L. and Johnson, J. H., *Unsteady vaporization histories and trajectories of fuel drops injected into swirling air*, SAE Paper 598C (1962).

[2] Chrigui, M., *Eulerian-Lagrangian Approach fot Modeling and Simulations of Turbulent Reactive Multi-Phase Flows under Gas Turbine Combustor Conditions*, PhD thesis, Technische Universitat Darmstadt, 2005.

[3] Faeth, G. M., *Evaporation and Combustion of Sprays*, Prog. Energy Combust. Sci. 9:1-76 (1983).

[4] Gosman, A., and Ioannides, E., *Aspects of computer simulation of liquid-fueled combustors*, Journal of Engineering 7:482-490 (1987).

[5] Hansell, D., Kennedy, I. M. and Kollmann, W., *A simulation of particle dispersion in a turbulent jet*, Int. Journal of Multiphase Flow 18-4:559-576 (1992).

[6] Koch, R., *Spray combustion*, In VKI lecture series: Turbulent combustion (March 2011).

[7] Kralj, C., *Numerical Simulation of Diesel Spray Processes*, PhD thesis, Imperial College London, 1995.

[8] Liu, Z., Zheng, C. and Zhou, L., *A joint PDF model for turbulent spray evaporation/combustion*, Proceedings of the Combustion Institute 29:561-568 (2002).

[9] Menter, F. R., *Zonal Two Equation $k-\omega$ Turbulence Models for Aerodynamic Flows*, AIAA Paper 93-2906 (1993).

[10] Patankar, S., *Numerical Heat Transfer e Fluid Flow*, Hemisphere Pub. Corp. McGraw-Hill, 1980.

[11] Ranz, W. E., and Marshall, W. R., *Evaporation from drops*, Chem. Eng. Prog 48-3:141-146 (1952).

[12] Sommerfeld, M. and Qiu, H.-H., *Detailed measurements in a swirling particulate two-phase flow by a phase-Doppler anemometer*, Int. Journal of Heat and Fluid Flow 12-1:20-28 (1991).

[13] Sommerfeld, M. and Qiu, H.-H., *Characterization of particle-laden, confining swirling flows by phase-doppler anemometry and numerical calculation*, Int. Journal of Multiphase Flow 19-6:1093-1127 (1993).

[14] Sommerfeld, M. and Qiu, H.-H., *Experimental studies of spray evaporation in turbulent flow*, Int. Journal of Heat and Fluid Flow 19:10-22 (1998).